Robotics Research Technical Report

Generatorium omnis laboris ex machina

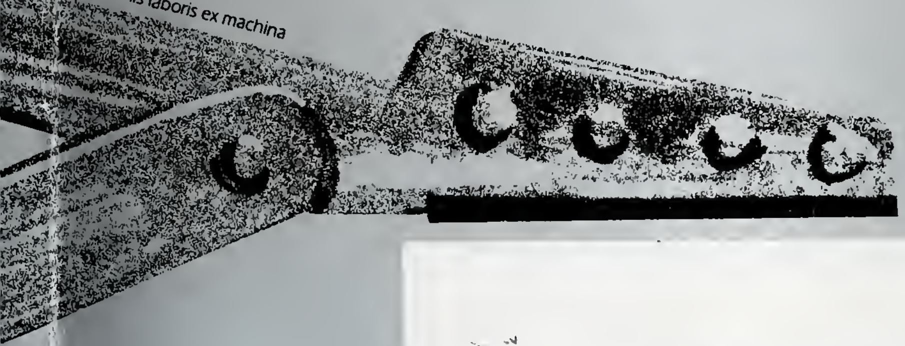

NEW YORK UNIVERSITY
COURANT INSTITUTE-LIBRARY
251 Mercer St. New York, N.Y. 10012

A Proposed Slip and Texture Sensor

by

Graham Walker

Technical Report No. 207
Robotics Report No. 66
March, 1986

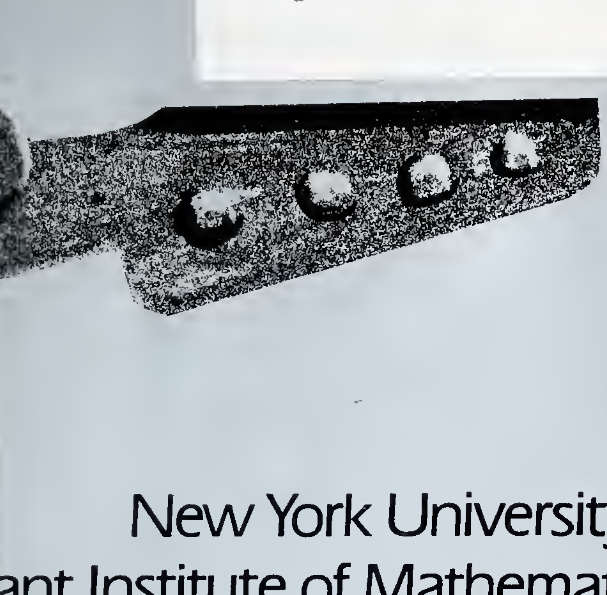

NYU COMPSCI TR-207 c.1
Walker, Graham
A proposed slip and texture sensor.

New York University
ant Institute of Mathematical Sciences

Computer Science Division
251 Mercer Street New York, N.Y. 10012

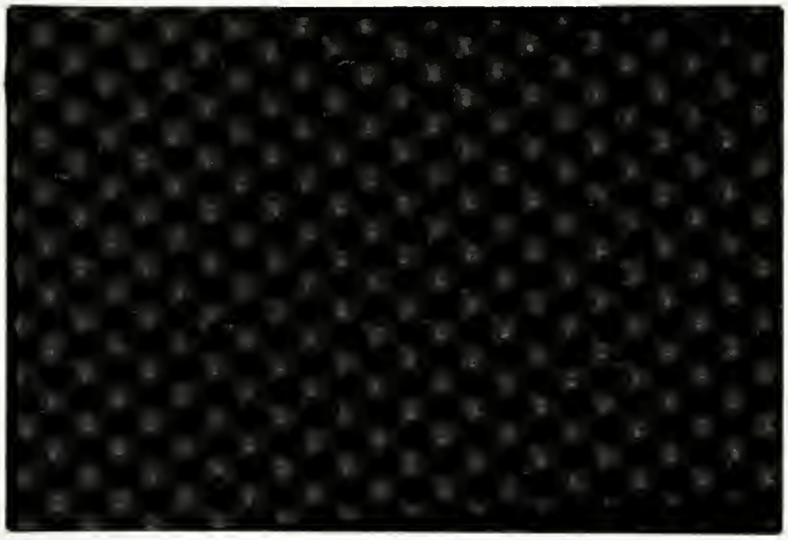

NEW YORK UNIVERSITY
COURANT INSTITUTE-LIBRARY
251 Mercer St. New York, N.Y. 10012

A Proposed Slip and Texture Sensor

by

Graham Walker

Technical Report No. 207
Robotics Report No. 66
March, 1986

New York University
Dept. of Computer Science
Courant Institute of Mathematical Sciences
251 Mercer Street
New York, New York 10012

Work on this paper has been supported by Office of Naval Research Grant N00014-82-K-0381, National Science Foundation CER Grant DCR-83-20085, and by grants from the Digital Equipment Corporation and the IBM Corporation.

A Proposed Slip and Texture Sensor*

by

Graham Walker

1. Introduction

Almost all of the tactile research that has been done to date has been associated with the design of sensors that would allow the shape of objects to be determined by touch alone (Larcombe[1], Taylor et al.[2], Raibert et al.[3] and Bardelli et al.[4]). This has resulted in the development of three commercially available tactile sensors (from Lord Corp., Tactile Robot Systems and Barry Wright Corp.) that can provide information about the three dimensional shape of objects with which they are in contact. However, very little research has been done in the area of slip detection.

One reason for this is that in order to simplify control schemes it has been assumed that the robot exerts sufficient force to prevent slip. This assumption has been adequate for the simple pick-and-place type of routines that robots have been asked to do in the past. If, however, robots are asked to operate in an unknown environment with real-time feedback the ability to detect slip becomes important since this ability would allow robots to make use of friction in their control loops. An example of this would be where a robot has to pick up an object about which it knows nothing (i.e. it does not know how light, weak or brittle the object is) except its external shape and position. In this case, with a slip sensor, the robot could attempt to lift the object with a progressively stronger grasp until the sensor detects zero slip between the robot and the object. This would therefore ensure that the weakest grasp was employed to pick up the object.

The work that has been done in the area of slip detection (Minoru et al.[5] and Hackwood et al.[6]) has relied on detecting slip at a point which therefore implies that large arrays of sensors would be required to ensure that slip anywhere on a surface could be detected. This report, however, describes a possible type of sensor that would not only detect slip over a large area with a minimal number of sensors but would also allow the texture of the surface, that the sensor was in contact with, to be determined.

---

*Work on this paper has been supported by Office of Naval Research Grant N00014-82-K-0381, National Science Foundation CER Grant DCR-83-20085, and by grants from the Digital Equipment Corporation and the IBM Corporation.

2. Sensor Design

If the human hand is examined it can be seen that the skin on the finger tips is corrugated (i.e. our finger prints). This allows the hand to provide a firm grip, by creating effectively a large number of small suction cups on the finger tips. In addition, these corrugations, possibly also serve the purpose of inducing vibrations in the skin when pulled over a surface thereby allowing the Pacinian corpuscles, which can sense skin vibrations (Corker et al.[7]) to detect slip. In a robot hand a similar system could also be implemented by corrugating a sheet of rubber or plastic on one side and strain gauging the remaining smooth surface. If these corrugations were then pulled over a surface the vibrations in the corrugations would appear as oscillating point moments in the sheet, which would then in turn, produce an oscillating strain on the smooth surface of the sheet.

These oscillations would therefore indicate that slip had occurred, but, in addition the character of these vibrations would indicate the mode by which the corrugations were set into motion and therefore provide information about the texture of the surface that was in contact with the corrugations. On a closer examination of this problem it can be seen that there are basically only two modes by which this could be achieved; a friction induced mode or a roughness induced mode. In order to examine these two modes in more detail it is necessary to simplify the problem by reducing it to a single corrugation in two-dimensions that is fixed at both ends (Fig. 1).

2.1. Friction Induced Oscillations

In the case of the friction induced oscillations the initial displacement of the corrugation would be caused by the body, which would initially be in frictional contact with the corrugation, moving relative to the corrugation. The tip of the corrugation would then remain stationary relative to the body as long as the body's displacement remained less than the distance that the cantilevered corrugation would displace by if exposed to a force equal to the maximum static friction force that could exist between the body and the corrugation (x_{max}). However, once the body slips beyond this point the corrugation would not remain in contact with the body since the static friction force would be overcome, by a restoring force that would increase to a value greater than this due to the additional displacement of the corrugation. At this point the force acting on the corrugation, due to friction, would drop to the value of the kinetic friction and the corrugation would attempt to return to its unloaded position. If then, it is assumed that the corrugation is allowed to compress freely along its axis (i.e. its Young's modulus is assumed to be zero along its axis), then the equation that describes this motion (Eqn. 1 and 2) can be derived from a simple force analysis (Fig. 2).

$$m\ddot{x} = F_f - kx, \quad \text{with } \dot{x}=0 \text{ at } x=x_{\mathrm{max}} \tag{1}$$

$$\dot{x}_{\mathrm{max}} = \frac{(F_f - kx_{\mathrm{max}})^2}{mk} \tag{2}$$

If the maximum attainable velocity of the corrugation ($\dot{x}_{\mathrm{max}}$) is less than the velocity of the moving body (V) then this motion would be continuous. However, if the maximum attainable corrugation velocity is greater than the body velocity the corrugation would eventually stop relative to the body at the point where these velocities are equal. The static friction would then once again become dominant and therefore cause the corrugation to be returned linearly to its maximum deflection position. In both of these case a periodic motion would therefore be established which would, in turn, produce a periodic strain on the smooth surface of the corrugated sheet.

2.2. Roughness Induced Oscillations

In the case of the roughness induced oscillations the initial displacement of the corrugation would be caused by the roughness hooking onto the corrugation and pulling it away from its rest position (Fig. 3). At some point the corrugation would then be displaced to such an extent that it will free itself from the roughness and attempt to return to its rest position. The corrugation would then vibrate freely, as described by Eqn. 3, until once again it came into contact with the next peak in the roughness.

$$m\ddot{x} = -kx, \quad \text{with } \dot{x}=0 \text{ at } x=x_{\mathrm{max}} \tag{3}$$

At this point the corrugation would then be returned linearly to its position of maximum deflection. If the roughness is then regarded as being periodic it can be seen that the oscillation of the corrugation and consequently the strain on the smooth surface of the corrugated sheet would be periodic.

3. Texture Sensing

If a strain gauge were then bonded to the smooth surface of the corrugated sheet it would be possible to detect slip by detecting a periodic strain in the gauge, that had a frequency equal to that of the cantilevered corrugation's natural frequency (Eqn. 4).

$$\omega_n = 3.52\left(\frac{EI_c}{\upsilon h^4}\right)^{\frac{1}{2}} \tag{4}$$

If, however, such a strain is further analysed by transforming it into the frequency domain, by using a Fourier transform (Eqn. 5), it would be possible to obtain texture information by examining the character of the spectrum.

$$G(\omega) = \int_{-\infty}^{\infty} g(t).e^{-i\omega t}dt \tag{5}$$

In particular, since the strains would be periodic, the spectrum would be a discrete function, with the spacing between the discrete point being equal to the frequency of the signal's overall periodicity (i.e. T_w). To observe the other features of the spectrum that are associated with textural information it is necessary to analyse a typical signal (Fig. 4). This signal, which is in effect the sum of a part cosine and a part line, can be described in the following form (Eqn. 6):

$$g(t) = \Big(u(t-NT_w) - u(t-(NT_w+T_s))\Big).\Big(a_1\cos(\omega_n t)+a_2\Big) +$$

$$\Big(u(t-(NT_w+T_s)) - u(t-(N+1)T_w)\Big).\left(\frac{a_1+a_2-(a_1\cos(\omega_n T_s)+a_2)}{(T_w-T_s)}(t-(N+1)T_w) + a_1 + a_2\right)$$

$$\text{where } N=0,1,2,3,\ldots\ldots \tag{6}$$

where $u(t)$ is the step function. When this equation is transformed into the frequency domain (Fig. 5) it can be seen that both the resulting real (Eqn. 7) and imaginary (Eqn. 8) parts of the spectrum possess peaks at points that are a function of the signal's overall periodicity (T_w) and the periodicity (T_s) of the part cosine.

$$G_r(\omega) = \frac{2a_1(\omega\cos(\omega_n T_s).\sin(\omega T_s) + \omega_n\sin(\omega_n T_s).\cos(\omega T_s))}{(\omega^2 - \omega_n{}^2)} + \frac{A(\cos(\omega T_w) - \cos(\omega T_s))}{\omega^2}$$

$$+ \frac{(a_2+AT_s+B).\sin(\omega T_s) + (AT_w-B).\sin(\omega T_w)}{\omega} \tag{7}$$

$$G_i(\omega) = \frac{a_1(\omega(\cos(\omega_n T_s).\cos(\omega T_s)-1) + \omega_n\sin(\omega_n T_s).\sin(\omega T_s))}{(\omega^2 - \omega_n{}^2)} + \frac{A(\sin(\omega T_s) - \sin(\omega T_w))}{\omega^2}$$

$$+ \frac{(a_2-AT_s+B).\cos(\omega T_s) + (AT_w-B).\cos(\omega T_w) - a_2}{\omega} \tag{8}$$

$$\text{where} \quad A = \frac{a_1 + a_2 - (a_1\cos(\omega_n T_s) + a_2)}{(T_w - T_s)} \quad \text{and} \quad B = AT_w - a_1 - a_2 \tag{9}$$

As a result of this analysis it can be seen that these two signal characteristics, which effectively provide textural information, would be more easily obtained from the frequency signature, which would only involve peak detection, rather than from the time signature, which would involve trying to judge where the time signal changed from being sinusoidal to linear, in nature. In addition, the zero crossings of the frequency signatures could also be used to ascertain T_w and T_s.

4. Practical Considerations

The time signals required to allow textural analysis to be performed could be obtained either from the sensor described by Hackwood et al.[6] or from a grid of strain gauges mounted to the smooth surface of the corrugated sheet (as described above). A grid of sensors, be they magnetoresistive or strain gauge, would also allow the slip velocity and direction to be measured by cross-correlating the time signals of two adjacent points (Eqn. 10) and measuring the temporal distance between adjacent correlation peaks. Or, if only the velocity were required, this could be obtained by merely auto-correlating an individual time signal (Eqn. 11) and once again measuring the distance between peaks.

$$\mathbf{R}_{12}(\tau) = \lim_{T\to\infty} \frac{1}{T_w} \int_{-T/2}^{T/2} g_1(\tau).g_2(t+\tau)dt \tag{10}$$

$$\mathbf{R}_{11}(\tau) = \lim_{T\to\infty} \frac{1}{T_w} \int_{-T/2}^{T/2} g_1(\tau).g_1(t+\tau)dt \tag{11}$$

However, if a grid of small sensors is used it would only be possible to detect slips on or close to one of the sensors in the grid. The result would therefore be that if it were necessary to detect slip over a large area either a very large number of sensors would be required, thus causing data acquisition problems, or some slip cases would not be detected. This problem can be alleviated by using a coarser grid of larger strain gauges, which would of course result in a loss of spatial resolution, but which would also allow each gauge to be able to detect slip over a much larger area, thereby greatly reducing the number of sensors required to monitor a large area for slip.

Both of the above strain gauge schemes would, of course be dependent on the existence of strains that would be large enough to be detected and in this respect an estimate of the magnitude of the largest strain is required. This can be achieved by calculating the magnitude of the maximum strain that would be produced by a single typical corrugation that is fixed at both ends (Fig. 6). >From an analysis of this model (Eqn. 12 and 13) it can be seen that the maximum moment that the smooth surface would be exposed to would be half the applied moment and therefore the resulting maximum strain would be approximately 900 x 10^{-6} (assuming that the Youngs modulus of the material is 1.0 kN/mm^2, the static coefficient of friction is 2.0 and the normal load on the corrugation is 1.5N).

$$M = \frac{M_c}{4} - \frac{3M_c}{2l}.x, \qquad \text{for } 0 \leq x \leq \frac{l}{2} \tag{12}$$

$$\epsilon = \frac{M.d}{2.E.I_s} \tag{13}$$

Since strains of this magnitude can be easily detected with equipment that presently exists it can therefore be seen that there would be sufficient strain available for either of these two strain gauge systems to be feasible. In addition to providing strains that were sufficiently large, any practical system would also have to provide signals that fluctuated at frequencies that were less than the response time of the instrumentation. In this respect the system described above would also meet this requirement, in that a typical corrugation (Fig. 6), which would have a total periodicity (T_w) and part cosine periodicity (T_s) of 522 μs (1.9 kHz) and 87 μs (11.5 kHz), respectively, would oscillate at frequencies that were less than the response time (40 kHz) of even an average instrumentation system.

It can therefore be seen, from the above example, that this sensor would allow a wide range of slip conditions and textures to be detected. In addition, if required, it would also be possible to construct a sensor that would be particularly sensitive to a specific set of conditions. This could be achieved by choosing a different combination of sheet dimensions and properties such as density, friction coefficients or Young's modulus; the most flexible of these being the Young's modulus which could be varied from 0.001 kN/mm^2 (soft rubber) to 200 kN/mm^2 (steel). However, it should also be noted that if dimensional changes are such that the sheet thickness to corrugation length ratio (d/h) becomes too small the above analysis would break down, in that the sheet would become the vibrating member whilst the corrugation would become merely a rigid member that transmitted the contact force to the sheet. In this case the general principle would still hold true but a new specific analysis would be required.

5. Future Work

This initial analysis of the corrugated slip detector has indicated that further work associated with this type of detector would prove to be extremely productive. It is therefore proposed that in order to extend this work the following list of tasks should be performed:

a) analyse how multiple corrugations would interact and thereby allow the multiple corrugation frequency signatures to be interpreted,

b) analyse the effect of random roughness on the time and frequency signatures,

c) analyse the result of cross- and auto- correlationing the time signals to determine the exact procedure required to obtain the velocity information,

d) conduct simple single corrugation experiments in order to examine the validity of the above analysis by not only examining the time but also the frequency signatures of the signals and

e) investigate any practical problems, such as the hysteresis and frictional damping within the corrugation material, that might have a bearing on the analysis.

6. References

1. Larcombe, M.H.E., "Tactile sensors, sonar sensors and parallax sensors for robot applications", 3rd Conference on **Industrial Robot Technology** , March 1976.

2. Taylor, P.M., Taylor, G.E., Kemp, D.J., Seim, J. and Pugh, A., "Software and hardware aspects of a sensory gripping system", **11th Conference on Industrial Robot Technology** , October 1981.

3. Raibert, M.H. and Tanner, J.E., "A VLSI tactile array sensor", **12th Conference on Industrial Robot Technology** , June 1982.

4. Bardelli, R., Dario, P., De Rossi, D. and Pinotti, P.C., "Piezo- and pyroelectric polymers skin-like tactile sensors for robots and prostheses", **13th Conference on Industrial Robot Technology** , April 1983.

5. Minoru, U., Iwata, K. and Shingu, H., "Tactile sensors for an industrial robot to detect slip", **2nd Conference on Industrial Robot Technology** , May 1972.

6. Hackwood, S., Beni, G., Hornak, L.A., Wolfe, R. and Nelson, T.J., "Torque-sensitive tactile array for robotics", **International Journal of Robotics Research 2** (2), 1983.

7. Corker, K., Mishkin, A. and Lyman, J., "Achievement of a sense of operator presence in remote manipulation", **Biotechnology Laboratory Technical Report 60** , University of California, Los Angeles, October 1980.

7. Nomenclature

a_1 - constant

a_2 - constant

A - constant

b - thickness of the corrugation

B - constant

E - Youngs modulus

F_f - friction force (static or kinetic)

F_1 - reaction force

F_2 - reaction force

$g(t)$ - time signature

$g_1(t)$ - time signal at point 1

$g_2(t)$ - time signal at point 2

$\mathbf{G}(\omega)$ - frequency signature

$\mathbf{G}_r(\omega)$ - real part of the frequency signature

$\mathbf{G}_i(\omega)$ - imaginary part of the frequency signature

h - length of the corrugation

i - $\sqrt{-1}$

I_c - second moment of area of the corrugation

I_s - second moment of area of the sheet

k - spring constant

l - length of the sheet

m - mass of the corrugation

M - moment

M_c - moment produced by the corrugation

M_1 - reaction moment

M_2 - reaction moment

N - a whole number

$\mathbf{R}_{11}(\tau)$ - auto-correlation function

$\mathbf{R}_{12}(\tau)$ - cross-correlation function

S - distance between the roughness peaks

t - time variable

T_s - part cosine periodicity

T_w - total periodicity

x - space variable

$u(t)$ - step function

V - sheet velocity

τ - dummy time variable

υ - mass per unit length

ω - radial frequency

ω_n - natural radial frequency

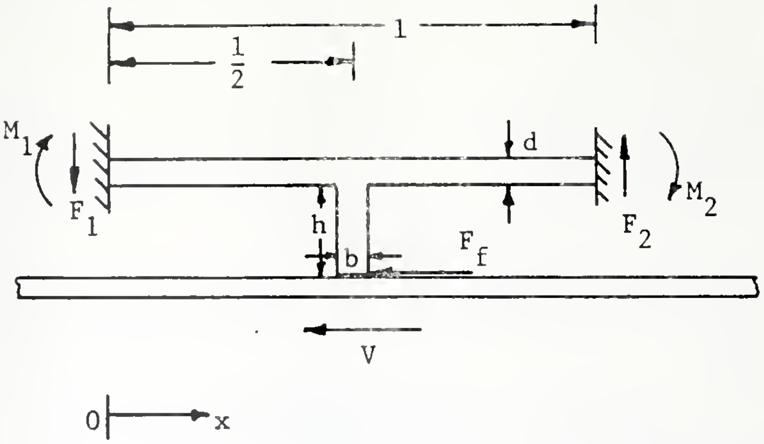

Fig. 1 The two-dimensional model of a surface passing under a corrugation.

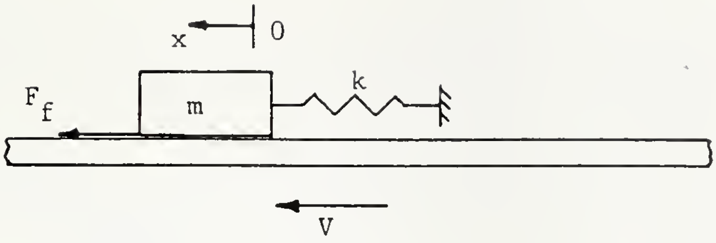

Fig. 2 A model of the corrugation deflection caused by surface friction.

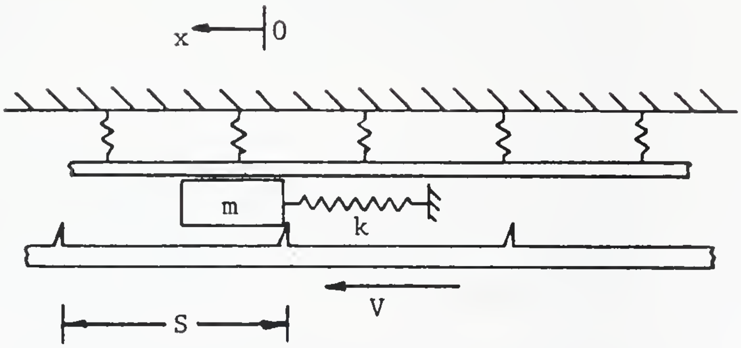

Fig. 3 A model of the corrugation deflection caused by surface roughness.

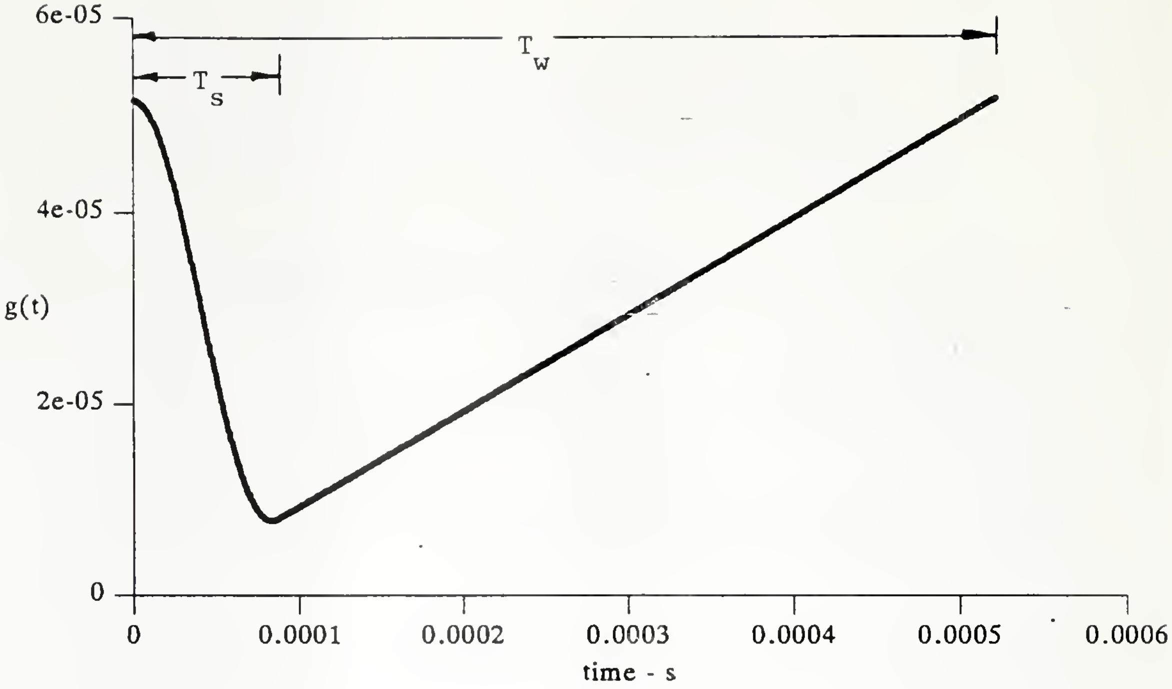

Fig. 4 A typical total oscillation associated with the friction induced mode.

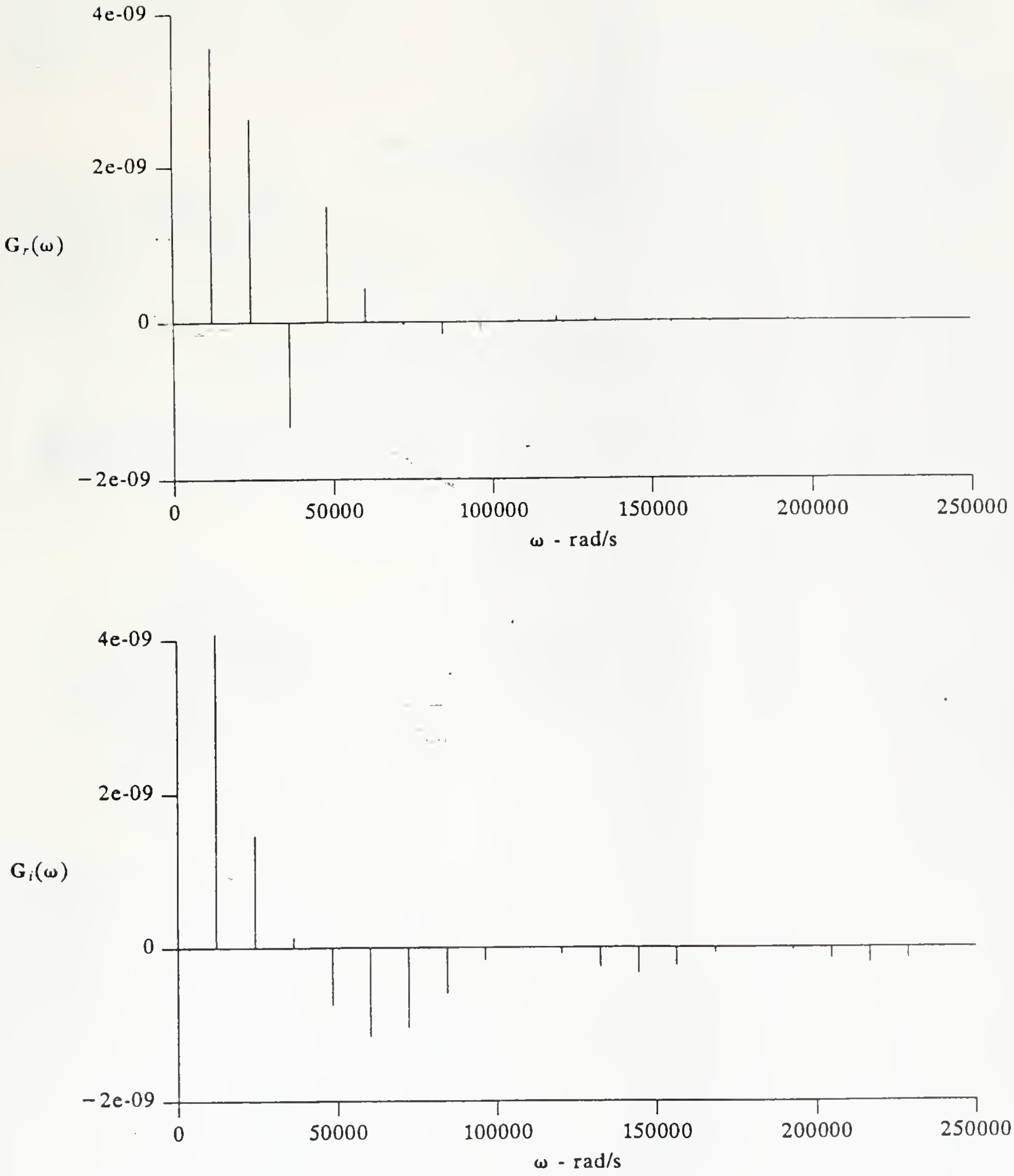

Fig. 5 The real and imaginary parts of a spectrum of an oscillation associated with the friction induced mode.

Static friction coefficient - 2.0
Kinetic friction coefficient - 1.15
Youngs modulous - 1.0 kN/mm^2
Density - 1200 kg/m^3
Width - 15 mm

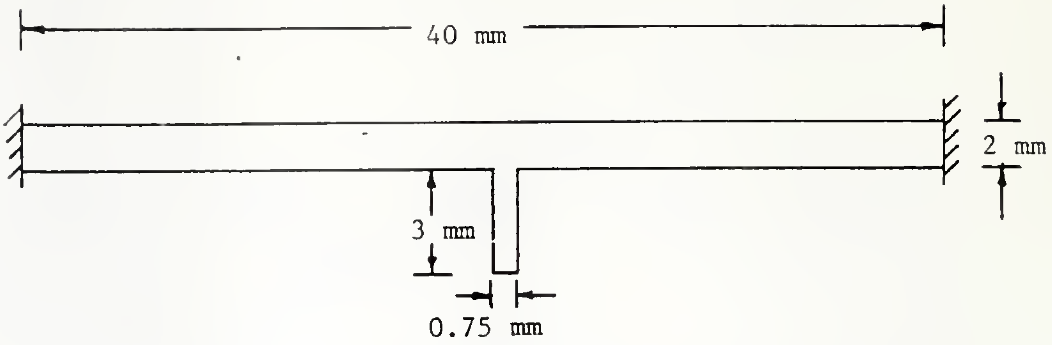

Fig. 6 The dimensions of a typical single corrugation.

NYU COMPSCI TR-207 c.1
Walker, Graham
A proposed slip and texture
sensor.

NYU COMPSCI TR-207 c.1
Walker, Graham
A proposed slip and texture
sensor.

LIBRARY
N.Y.U. Courant Institute of
Mathematical Sciences
251 Mercer St.
New York, N. Y. 10012

This book may be kept JUL 16 1986
FOURTEEN DAYS
A fine will be charged for each day the book is kept overtime.

GAYLORD 142 PRINTED IN U.S.A.